Journal of Membrane Science 694 (2024) 122430

Contents lists available at ScienceDirect

Journal of Membrane Science

journal homepage: www.elsevier.com/locate/memsci

# Techno-economic analysis of carbon molecular sieve membranes to produce oxygen enrichment air

Tiago Araújo [a,b], Telmo da Silva Lopes [a,b], Gabriel Bernardo [a,b], Adélio Mendes [a,b,*]

[a] LEPABE - Laboratory for Process Engineering, Environment, Biotechnology and Energy, Faculty of Engineering, University of Porto, Rua Dr. Roberto Frias, 4200-465, Porto, Portugal
[b] ALiCE - Associate Laboratory in Chemical Engineering, Faculty of Engineering, University of Porto, Rua Dr. Roberto Frias, 4200-465, Porto, Portugal

ARTICLE INFO

*Keywords:*
Carbon capture
Membranes
Carbon membranes
Oxygen enrichment from air
Separation cost

ABSTRACT

Oxygen Enriched Air (OEA) is essential for medical applications, metal production, chemical production, the petrochemical industry, and energy processes. In this work, carbon molecular sieve membranes (CMSM) and membrane systems are analyzed concerning their technical and economic feasibility to produce OEA for medical, post-combustion, and oxy-combustion applications. Process parameters, such as stage-cut, feed-to-permeate pressure ratio, membrane area, and the number of stages, were studied to assess the technical and economic feasibility of this technology. In this work, it was observed that for each membrane, there is a permeating oxygen concentration that minimizes the specific oxygen cost. The production of 56 $tonO_2 \cdot day^{-1}$ for a combustion enhancement process with a concentration of 72 % was obtained in a single-stage with a specific cost of 61.0 $€ \cdot tonO_2^{-1}$. A single-stage is also effective for producing OEA for medical applications (required concentration of 82 %) at a minimum separation cost of 45.8 $€ \cdot tonO_2^{-1}$. However, a two-stage system is required to produce OEA with a concentration higher than 95 % for oxy-combustion with an OEA production cost of 83.8 $€ \cdot tonO_2^{-1}$. These production costs are lower than those obtained with two different commercial membranes and are competitive with medium-scale cryogenic distillation and pressure swing adsorption processes.

## 1. Introduction

Oxygen-enriched air (OEA), or air with more than 21 vol% of oxygen, has long been recognized as an important commodity with applications in various industries [1–3]. These include chemical [4], food [5], healthcare [6,7], petrochemical [8], wastewater treatment [9], steel-making [10], and more recently, oxy-combustion. In the healthcare industry, oxygen is an essential medicine used in different concentrations [11]. With the onset of the COVID-19 pandemic, its usage has substantially increased as a therapy for treating respiratory diseases [12]. In the same way, the use of OEA as an oxidizing agent in combustion-based processes is also on the rise [1]. In such a process, fuels are oxidized traditionally using oxygen with a concentration higher than 95 %, instead of air, producing the desired heat and, ideally, only carbon dioxide and water vapor as by-products, including no NOx. The nitrogen present in the air consumes latent heat, which is later wasted through the flue gas emissions; using air diminishes the overall efficiency of the combustion process and produces undesirable by-products such as CO and NOx [13]. In contrast, the use of OEA as an oxidizing agent improves the overall energy efficiency of the process in several ways [14]: (1) the process achieves more complete combustion; (2) there is a better use of the available oxygen; (3) heat transfer rate to the boiler increases; (4) the amount of heat loss through flue gas decreases since nitrogen is not fed together with oxygen; and (5) the overall amount and variety of pollutants emitted is lower [1,2,14]; and (6) overall fuel consumption decreases substantially especially for higher operating temperatures. The oxy-combustion is more attractive as the fuel price rises, the $CO_2$ recovery becomes required, and the production costs of OEA decrease [15].

The increase in OEA demand has rekindled the interest in developing new and more efficient technologies that can deliver such a product. Currently, OEA is mainly produced by three processes: cryogenic distillation [16], pressure swing adsorption (PSA) [17], and membrane separation [1]. Cryogenic distillation is the most established method and is employed in plants where high purity (>99 % $O_2$) and high flowrates (100–300 $tonO_2 \cdot day^{-1}$) are required [5]. Its energy consumption varies

* Corresponding author. LEPABE - Laboratory for Process Engineering, Environment, Biotechnology and Energy, Faculty of Engineering, University of Porto, Rua Dr. Roberto Frias, 4200-465, Porto, Portugal.
*E-mail address:* mendes@fe.up.pt (A. Mendes).

https://doi.org/10.1016/j.memsci.2024.122430
Received 19 October 2023; Received in revised form 19 December 2023; Accepted 7 January 2024
Available online 10 January 2024

from *ca.* 75 to 275 kWh·ton$O_2^{-1}$ depending on the desired oxygen concentration [18]. However, some drawbacks of cryogenic distillation are the high capital investment and the high energy consumption. PSA can be employed as an alternative to cryogenic separation; its separation mechanism is based on the adsorption equilibrium [19,20]. PSA units produce high-concentration $O_2$ (*ca.* 95 % balanced mostly with argon) with a production rate that normally goes from 1 to 100 ton$O_2$·day$^{-1}$ [5], consuming between 360 and 500 kWh of energy per ton$O_2$. Production costs range between 40 and 50 €·ton$O_2^{-1}$ for a production rate between 1 and 50 ton$O_2$ per day [1]. This process is also considered energy intensive and has a moderate capital cost, making it unappealing for low (<10 ton$O_2$ per day) and high production rates (>300 ton$O_2$ per day) [21]. Due to the inherent disadvantages of the two most employed OEA production technologies, there is clearly a market opportunity for processes that prove to be cheaper and energy efficient for intermediate production rates, between 20 and 300 ton$O_2$·day$^{-1}$ [22]. It should be emphasized that water electrolysis can also be used to produce OEA. However, this process is only attractive when hydrogen is the desirable product and for applications in the neighboring electrolysis plant [23].

In recent years, membranes have become a standout technology in the gas separation market, especially for the small-to-medium scale applications [1,5]. Separation membranes can be made of polymeric or inorganic materials, such as carbon, ceramics, or metals. They do not require a regeneration step, they have a straightforward design and a small environmental impact, and they are modular - making them more easily scalable and flexible [24]. Additionally, this technology does not use chemicals, generates no waste, the gas products can be directly used or discharged, and membranes have a minimal equilibration time that makes them suitable for fluctuating feed flow rates [25]. In the separation process, membranes are usually placed inside a modular incasing (module) with different types of configurations: flat plate, tubular, and hollow fiber. The module can be tubular, planar, or spiral wound [24]. In the hollow fiber membrane configuration, thousands of membranes can be packed inside a small volume, maximizing the packing density (*i.e.*, the largest active membrane area in relation to the module volume) [26]. Since gases display normally low viscosities, this configuration is normally preferred for producing OEA.

The first commercial membrane for gas separation was by Monsanto, the PRISM® separators (now owned by Air Products), for the hydrogen purification [27]. However, Generon® separator by Dow, was the first membrane technology for air separation with a large market penetration [28]. Initially proposed in the 1980s, the membrane separation technology was specifically developed to produce nitrogen-enriched air (NEA) for applications that require inert atmospheres. Since then, several membrane solutions for producing nitrogen-enriched air have been commercialized, notably by Air Products and Linde [24,25]. Still, in the 1980s decade, techno-economic studies indicated that the use of polymeric membranes for oxygen-enriched air production [31], was only competitive for small production scale, between 10 ton$O_2$·day$^{-1}$and 25 ton$O_2$·day$^{-1}$, and for an $O_2$ concentration between 25 % and 40 % [28]. More recently, in 2014, Belaissaoui et al. [18] reached a similar conclusion, considering modern materials displaying an $O_2/N_2$ selectivity between 4.5 and 6. The membrane processes display a selectivity-permeability tradeoff first described by Robeson, who reported for the first time the so-called Robeson's upper bound plots [29]. This intrinsic limitation means that high-purity and high production rates are only possible with the addition of several separation stages, increasing the overall cost of the membrane separation process [5]. As pointed out by Belaissaoui, for intermediate purities, new membrane technologies such as carbon molecular sieve membranes (CMSMs) can be quite competitive since they usually present much higher separation performances [18].

Intermediate-purity oxygen can be especially useful in combustion-enhancement applications [1,5,8,14]. As previously discussed, using OEA in non-electrifiable processes can significantly improve the environmental, and economic performance in industries such as glass, ceramics, or electricity production [1]. The oxy-combustion consists of introducing high-purity OEA (≥95 % of $O_2$) into a furnace/boiler, which largely improves the efficiency-related metrics of the reaction, produces a $CO_2$-enriched flue gas, and decreases the production rate of pollutants such as NOx and CO. However, as pointed out by the US Department of Energy (USDOE), intermediate-purity oxygen-enriched air – between 45 % and 60 % – is already enough to decrease fuel consumption by over 30 %, for a flame temperature of *ca.* 1100 °C [30]. Besides, the flue gas already has a higher concentration of $CO_2$ (though lower than in the oxy-combustion scenario), making its post-combustion separation/capture more economically attractive.

In a recent publication, K. Ahrawal and his team explored these two scenarios, using membranes to produce high/intermediate purity oxygen from air [1]. The cost saving of supplying an oxygen-enriched air stream with 30 % of $O_2$ to feed a natural gas-fired furnace (293 kWh), allows an energy saving of 40 % [13]. An increase in the selectivity of the membrane did not interfere with the energy savings of the combustion process, but the increase in permeance enabled the production of a higher purity OEA, *i.e.* 50 % of $O_2$, allowing an energy saving of 60 %. A post-combustion $CO_2$ capture was also analyzed for this furnace. The energy required for capturing and purifying the flue gas of a furnace fed with an OEA stream with 65 % of oxygen was estimated to be 0.98 MJ·kg$CO_2^{-1}$, which results in a $CO_2$ capture cost of *ca.* 40 €·kg$CO_2^{-1}$ [1].

Similarly, a techno-economic study by Adhikari et al. [5], demonstrated that two stages of (polymeric) membranes with a selectivity of 5.5 and a permeance of 1000 GPU would be needed to produce 90 % pure OEA to perform oxy-combustion in a small-scale coal gasification process (5 MWe). Although the predicted separation cost (50 €·tonOEA$^{-1}$) was competitive with cryogenic distillation (45 €·tonOEA$^{-1}$) and PSA (65 €·tonOEA$^{-1}$), currently, there are no membranes available on the market that can achieve this separation performance. This study highlights the need for researchers to develop new membrane materials with performance metrics that can meet these requirements. In particular, increasing the permeance seems to be imperative since the cost of generating OEA significantly decreases as this metric increases.

CMSM are an emerging class of membranes that have shown separation performances well above Robeson's upper bound for polymeric membranes. Another great advantage of these membranes is their proven stability in contact with corrosive and high-temperature environments [31]. In particular, membranes prepared from a cellulose precursor are the ones that seem to be the most economically attractive due to their exceptionally high separation performance, relatively low production cost, and easily scaled-up production procedures. In 2018, Haider et al. [32], demonstrated the use of a CMSM prepared from cellulose ($O_2/N_2$ selectivity of 18) capable of producing, in a single stage, a stream with *ca.* 73 % of oxygen from air with a separation cost of 80 €·ton$O_2^{-1}$. Our research group prepared a CMSM from a cellulose precursor modified with urea that exhibits a permeability to oxygen greater than 330 barrer and an $O_2/N_2$ selectivity greater than 52 [33].

Motivated by the latest developments on very high-performing CMSMs for $O_2/N_2$ separation, this work makes a techno-economic analysis on using these membranes to produce oxygen-enriched air for health (oxygen concentration of >82 %), oxy-combustion (oxygen concentration of >95 %), and combustion-enhancement (oxygen concentration of >65 %) applications.

## 2. Model equations

The gas permeation in a carbon molecular sieve membrane is well described by the sorption-diffusion model [34]. Therefore, the membrane permeability is the product between sorbed-phase diffusivity and the sorption coefficient of each gas component: $P_i = S_i D_i$. This model assumes that the sorption coefficient is governed by Henry's law ($c_i = S_i p_i$). The permeation rate of the membrane can then be written as:

$$J_i = -D_i\frac{dc_i}{dz} = S_i D_i\frac{dp_i}{dz} = P_i\frac{\Delta p_i}{\ell} \quad (1)$$

where $D_i$ is the diffusion coefficient for component $i$, $c_i$ is the sorbed concentration of $i$, $z$ is the axial coordinate of the membrane thickness, $S_i$, is the sorption coefficient of component $i$, $p_i$ is the partial pressure of component $i$, $P_i$ is the permeability to component $i$ and $\ell$ is the membrane thickness. The ratio between permeability and thickness of the membrane is the permeance, $L_i$.

A simple method for solving counter-current membrane models discretized into $n$ equal-area perfectly mixed stages – *cf.* Fig. 1. The differential molar flow for each component, $i$, on the retentate side is given by:

$$dF_{i,R} = L_i\left(p_R x_{i,R} - p_P y_{i,P}\right)dA \quad (2)$$

where $F_{i,R}$ is the molar flow of $i$ in the retentate side, $L_i$ is the permeance ($L_i = P_i/\ell$), $p_R$ is the retentate pressure, $p_P$ is the permeate pressure, $x_{i,R}$ is the molar fraction of $i$ in the retentate side, $y_{i,P}$ is the molar fraction of $i$ in the permeate side increment, $z$ is the dimensionless space coordinate and $dA = \pi\, d\,\ell\, dz = A\, dz$ is the membrane area, where $d$ is the hollow fiber diameter and $z$ is the axial position along the hollow fiber. The permeate and the retentate flow in opposite directions:

$$\frac{dF_{i,R}}{dz} = \frac{dF_{i,P}}{dz} \quad (3)$$

A system of non-linear differential equations needs to be solved. Due to the complexity of such a task, an initial condition of the concentration profile at the permeate side needs to be provided [35,36]. In addition, one boundary condition is needed for each first-order differential equation. In this work, the following boundary conditions were considered for the retentate side:

$$z = 1: \quad F_R = F_{feed} \quad (4)$$

$$x_{i,R} = x_{i,feed} \quad (5)$$

and for the permeate side without sweep gas flow:

$$z = 0: \quad F_P = 0 \quad (6)$$

Different approaches can be used to solve this counter-current model, namely: (1) Coker et al. (1998) – successive stages method with tridiagonal matrices using the Thomas algorithm [37]; (2) Cruz et al. (2005) – finite volume method with high-resolution scheme with a false transient method using the LSODA package [36]; and (3) Grainger et al. (2007) – iterative method with pressure increments on the permeate side [38]. In this work, the set of differential equations are solved simultaneously using *bvp4c* function from Matlab®. The *bvp4c* function integrates a system of differential equations of the form $y' = f(x,y)$, subject to the boundary condition [39].

In the implementation of this model, a set of assumptions were made, namely: plug flow without axial dispersion; ideal gas behavior; the permeability values are assumed to be independent of temperature and pressure; negligible concentration polarization; no pressure drop on both sides of the membrane; negligible membrane deformation under pressure and no radial velocity profile. The simulator validation can be found in Table S1 of the Supplementary Note 1.

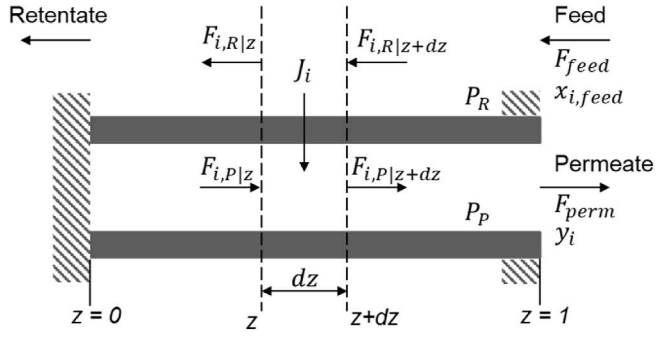


**Fig. 1.** Scheme of an ideal configuration of a hollow fiber membrane and its mass balance at an infinitesimal volume.

## 3. Simulation basis

As previously referred, this work aims to understand if the recent developments in CMSMs for $O_2/N_2$ separation can make this technology attractive for OEA applications, namely using the permeation parameters reported in Ref. [33]. For comparison proposes, the commercial membrane Polaris™ – Membrane Technology and Research – and membrane Prism® – Air Products, were also considered, besides none of them being used for oxygen enriched air production [40,41]. The separation parameters considered for the three different membranes are indicated in Table 1.

The permeabilities to pure components and to $O_2/N_2$ mixtures are very similar since these two gases display similar adsorption isotherms on cellulose-based CMSM [33,42]. Air is mostly composed of nitrogen – 78 %, oxygen – 21 % and argon – 0.9 %. However, argon displays a permeation rate closer to nitrogen [43–45], and for simplicity, the air mixture is often assumed to be composed only of oxygen – 21 % and nitrogen – 79 %.The gas permeance unit (GPU), corresponds to $3.35 \times 10^{-10}$ mol m$^{-2}$ s$^{-1}$•Pa$^{-1}$. For the CMSM, it was assumed a selective layer thickness of 3 μm. The normalized permeate oxygen flowrate (ratio between the permeating oxygen and the air feed flow rates – productivity) and the specific membrane area ($\varphi$, the ratio between the membrane area and the feed flow rate) were obtained for a single-stage carbon membrane module, for a constant feed-to-permeate pressure ratio ($R = P_{feed}/P_{permeate}$) of 100 – Fig. 2. A study on the influence of the pressure ratio on the OEA production was then carried out.

For the techno-economic study, the specific membrane area was computed for a target oxygen production concentration; the production costs and energy requirements were then calculated. The stage-cut ($\theta = Q_{permeate}/Q_{feed}$) and the permeate concentration were computed. A design of experiments (DoE), based on the Response Surface Methodology (RSM) [46], was applied to determine the optimum operating and design conditions for the production of oxygen with 3 different concentrations (>70 %, >82 %, and >95 %); feed-to-permeate pressure ratio and specific membrane area were taken as factors – independent variables. The statistical software JMP ® (SAS Institute Inc.) was employed for this study. The specific oxygen cost – permeate flowrate times the oxygen concentration – was used for obtaining the optimized operating and design conditions. The dependent variables were interpolated using a second-order polynomials [46]. The selected domain of the independent variables are: the feed-to-permeate pressure ratio ($R$ = 10–100) and the specific area ($\varphi$ = 40–400 m$^2$·day·ton$^{-1}$); and, the stage cut, the oxygen concentration and the specific cost were the selected response variables ($\hat{y}$). The fitting equation is:

$$\hat{y} = \beta_0 + \beta_1\left(\frac{R-\overline{R}}{(R_{+1}-R_{-1})/2}\right) + \beta_2\left(\frac{\varphi-\overline{\varphi}}{(\varphi_{+1}-\varphi_{-1})/2}\right) + \beta_3\left(\frac{R-\overline{R}}{(R_{+1}-R_{-1})/2}\right)\left(\frac{\varphi-\overline{\varphi}}{(\varphi_{+1}-\varphi_{-1})/2}\right) + \beta_4\left(\frac{R-\overline{R}}{(R_{+1}-R_{-1})/2}\right)^2 + \beta_5 \bullet \left(\frac{\varphi-\overline{\varphi}}{(\varphi_{+1}-\varphi_{-1})/2}\right)^2 \quad (7)$$

**Table 1**
Separation performance of the membranes used in this work.

| Membrane | Permeance (GPU) | $O_2/N_2$ selectivity (−) |
|---|---|---|
| **Carbon membrane** | 111 | 54 |
| **Polaris™** | 220 | 5 |
| **Prism®** | 68 | 6.9 |

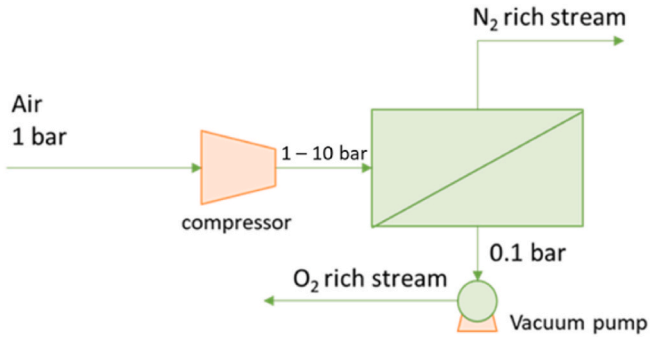


**Fig. 2.** Sketch of a single-stage membrane separation unit.

where, $\beta_i$ are the regression coefficients, $R$ is the feed-to-permeate pressure ratio, $\overline{R}$ is the domain average feed-to-permeate pressure ratio, $R_{-1}$and $R_{+1}$ are the limit feed-to-permeate pressure ratio values of the domain, $\varphi$ is the specific membrane area, $\overline{\varphi}$ is the intermediate specific membrane area between limiting areas $\varphi_{-1}$ and $\varphi_{+1}$. The significance of the parameters was characterized by the *p*-value. The model accuracy and fitness were accessed using the coefficient of determination ($R^2$) and the root mean square error (RMSE). A sensitivity analysis of the membrane thickness (selective layer) was carried out to assess its impact on the specific cost. The influence of the price of electricity and the project lifetime (capital amortization time) were also studied. Finally, the results obtained were compared with traditional oxygen production processes.

## 4. Cost model

The cost model used in this techno-economic assessment was adapted from previous publications [32,34,47,48]. The equipment considered in the simulations were the membrane skid, the compressors, and the vacuum pumps. The other components of the system (membrane capsule, piping, valves, heat exchangers, expanders, and transport pumps) have relatively low capital and operating costs compared to large equipment [32]; the capital expenditure (CAPEX) was then assumed to be only the sum of the cost of these main components. The cost of the polymeric membranes ($C_M$) is between 25 and 125 €·m$^{-2}$, and the cost of the CMSM was set to 100 €·m$^{-2}$ [32]. The cost of compressors and vacuum pumps was based on empirical relationships considering the power required by the compressor and vacuum pump, respectively [49]. The power of a compressor ($P_c$) is calculated by the following equation:

$$P_c = \frac{QRT}{\eta_c}\frac{k}{k-1}\left[\left(\frac{P_{\text{discharge}}}{P_{\text{suction}}}\right)^{\frac{k-1}{k}} - 1\right] \tag{8}$$

where $Q$ is the feed flow rate to the compressor, $\eta_c$ is the compressor efficiency (here assumed to be 85 %), and $k$ is the specific heat ratio (here assumed to be 1.4). For vacuum pump power ($P_{vp}$) was computed using the same equation but it was considered an efficiency of 60 % and 0.1 bar. The compressor and vacuum pump costs were calculated by the following equations [49,50]:

$$C_c = 5840 P_c^{0.82} \tag{9}$$

$$C_{vp} = 32500\left(\frac{1.341 P_{vp}}{10}\right)^{0.5} \tag{10}$$

For the CAPEX, a direct and indirect costs factor ($F$) of 20 % was considered, and a chemical engineering plant cost index ($C_{CEPCI}$) of 699.97 (2021) for the equipment was adopted for all inflation adjustments of 397 ($I$) [47]. The CAPEX was calculated by the following equation:

$$C_{CAPEX} = F \times \frac{C_{CEPCI}}{I} \times \left[C_M + C_c + C_{vp}\right] \tag{11}$$

The annual capital related cost ($C_{ACRC}$) was computed based on the capital costs amortization during the period of execution of the project; it was assumed an amortization of 10 years [34]. Regarding the operational-related expenditure cost ($C_{OPEX}$), only the electricity price of 0.08 €·kWh$^{-1}$ was considered, as the labor and utility costs are much smaller than this. The plant was assumed to operate 8000 h per year, and the energy cost was calculated from the following equation:

$$C_{OPEX} = C_{energy} = 0.08 \times \left(P_{vp} + P_c\right) \times 8000 \tag{12}$$

The specific cost of the OEA production was calculated from the ratio of "the sum of the annual capital related cost and OPEX" by "the annual oxygen enrichment production":

$$\text{Specific cost } (€ / \text{ton}O_2) = \frac{C_{ACRC} + C_{OPEX}}{Q_{O_2}} \tag{13}$$

where $Q_{O_2}$ (ton$O_2$·year$^{-1}$) is the mass production of oxygen, present in the OEA stream per year (ton$O_2$ per year).

## 5. Results and discussion

This techno-economic study assumes different separation scenarios, as indicated in Fig. 2, were considered. The role of the main operating variables is studied in detail, namely the influence of 1) feed flow rate; 2) pressure ratio; 3) oxygen concentration; and 4) sensitivity analysis.

### 5.1. Influence of the feed flow rate on the productivity and oxygen concentration

The normalized permeate oxygen flowrate (ratio between the permeate oxygen and the air feed flow rates – productivity) as a function of the oxygen concentration is plotted in Fig. 3A. The feed-to-permeate pressure ratio was kept at 100. As expected, the oxygen production rate decreases as the oxygen product concentration increases. The maximum oxygen concentration achieved in a single carbon membrane stage is 93 %. The permeate concentration increases as the stage cut decreases for a set pressure ratio, permeance, and $O_2/N_2$ selectivity values. When the stage cut onsets a fast decrease for reaching a given oxygen concentration, the nominal oxygen concentration is reached, which in this case was 93 % – pressure ratio: 100; permeability: 330 barrer, $O_2/N_2$ selectivity: 53, and the stage cut: 0.015). This maximum concentration corresponds to reaching the region of the membrane limited by selectivity. As the required membrane surface area increases, the oxygen product concentration decreases, and the product flowrate increases, as illustrated by Fig. 3B.

Fig. 4 shows the specific cost of oxygen-enriched air production as a function of oxygen product concentration (A) and oxygen recovery (B). Five different air feed rates (13, 25, 125, 250, and 623 ton of air per day) were considered to determine the required membrane area and respective specific cost and energy consumption. To perform the economic analysis, the feed pressure was maintained at 10 bar and the permeate pressure at 0.1 bar. Fig. 4A plots the specific oxygen production cost as a function of the oxygen product concentration; since CAPEX does not depend linearly on the feed flowrate, there is a curve for each feed flowrate. This figure indicates that the specific oxygen cost decreases for higher feed flowrates; more interestingly, it shows that the specific cost is mostly constant up to a threshold oxygen product concentration, which in this case is *ca.* 87 %. For example, for an air feed flowrate of 623 tons·day$^{-1}$, a product stream with an oxygen concentration of 87 % costs *ca.* 74€·ton$O_2^{-1}$, but a product stream with an oxygen concentration of 93 % costs 45 times more. The maximum oxygen concentration for a mostly constant specific cost value was named nominal oxygen concentration.

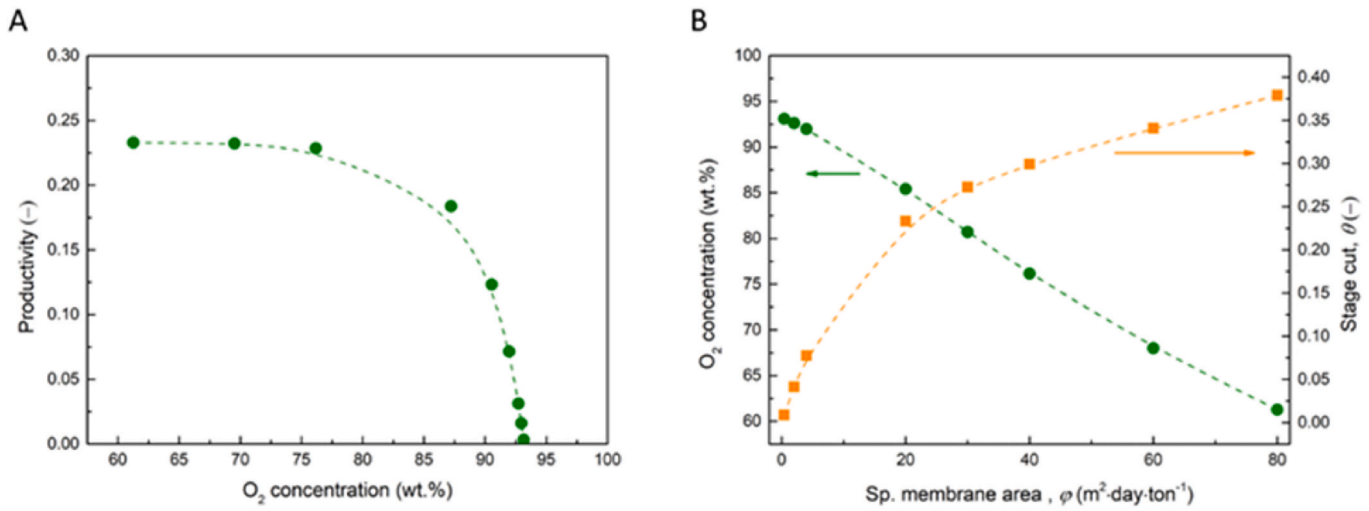


**Fig. 3.** (A) Normalized permeate oxygen flowrate as a function of the permeated oxygen concentration for a single-stage CMSM separator (productivity); (B) oxygen concentration and stage cut as a function of the specific membrane area. A feed-to-permeate pressure ratio of 100 was assumed. The lines were added to guide the eyes.

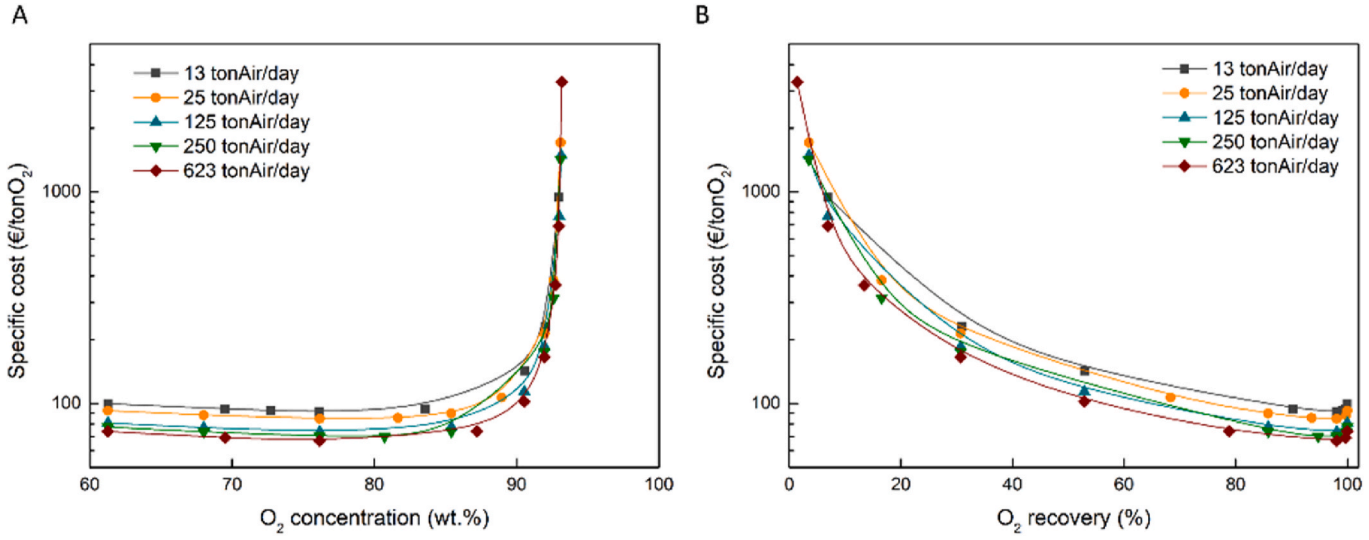


**Fig. 4.** Specific cost of the oxygen-enriched air stream as a function of (A) permeated oxygen concentration and (B) oxygen recovery for the 5 different plant capacities. The lines were added to guide the eyes.

### *5.2. Influence of the feed-to-permeate pressure ratio on the specific oxygen cost*

The influence of the feed-to-permeate pressure ratio ($R$) was studied as a function of the membrane area, oxygen concentration, and stage cut. Five different feed-to-permeate pressure ratios (10–100) were used. The oxygen concentration and the stage cut as a function of the specific membrane area for selected feed-to-permeate pressure ratios are plotted in Fig. 5.

From this study, it is possible to confirm that as the feed-to-permeate pressure ratio increases, the membrane area needed for the separation decreases. The curves of oxygen concentration as a function of the specific membrane area are linear. The oxygen concentration increases with the pressure ratio since the real selectivity increases with the feed-to-permeate pressure ratio [51]. The stage cut increases with the membrane area; as the pressure ratio increases, the membrane area required to obtain the same stage cut is smaller. It should be noted that for a feed pressure of 1 bar, a blower will need to be incorporated into the process to work and maintain the flow on the upstream side of the membrane.

To perform an economic analysis and calculate the influence of the pressure ratio on the specific cost and energy consumption of oxygen-enriched air production, the air feed flow rate (250 tons per day) and the permeate pressure (0.1 bar) were assumed constant. The simulations were conducted for 5 different feed pressures (1, 3, 5, 8 and 10 bar). A single stage of CMSM was assumed. For 1 bar of feed pressure, the compressor was not considered; a vacuum pump was used in all simulations.

The specific cost and specific energy consumed as a function of the oxygen concentration and recovery – ratio between the permeate oxygen and the feed oxygen flowrates – are shown in Fig. 6A–D. The specific cost of producing oxygen-enriched air is higher for higher pressure ratios. The specific oxygen cost as a function of the oxygen product concentration is the lowest for the lowest feed pressure *ca.* 85 % – nominal oxygen concentration. The specific cost decreases as the recovery increases (stage cut) due to the increased permeated flowrate. Nevertheless, there is an exception for 1 bar feed of pressure. In this case, the behavior deviates from this pattern because only the permeate stream is pumped using a vacuum pump – there is no feed compressor. The

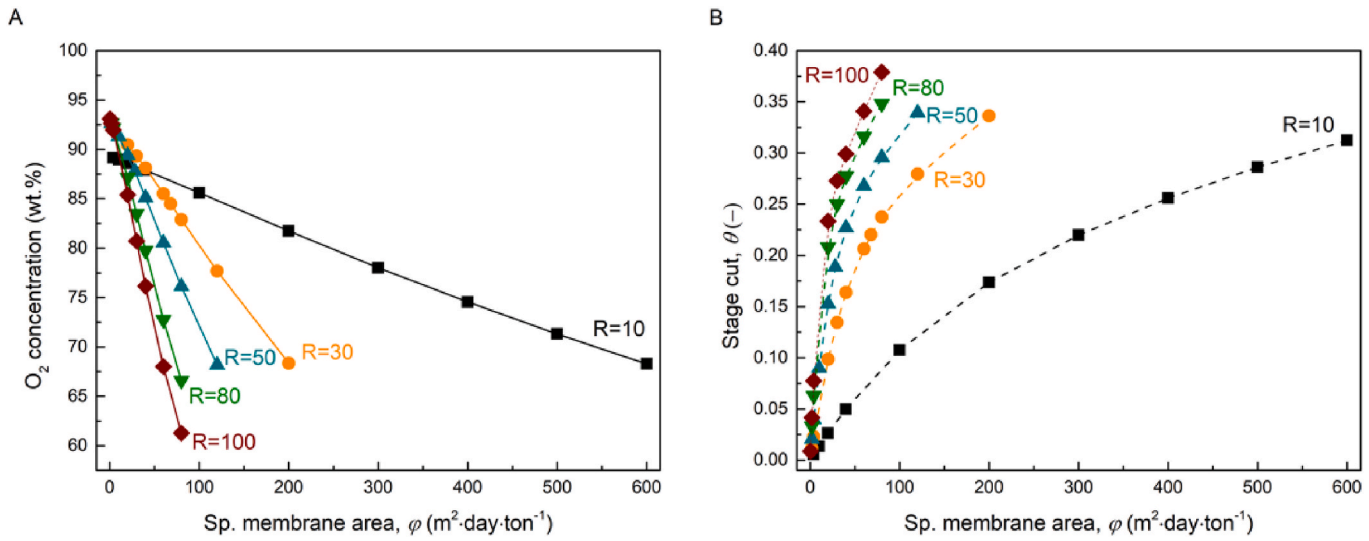


**Fig. 5.** (A) Oxygen concentration and (B) stage cut as a function of the ratio of the membrane area and feed flow rate (specific membrane area).

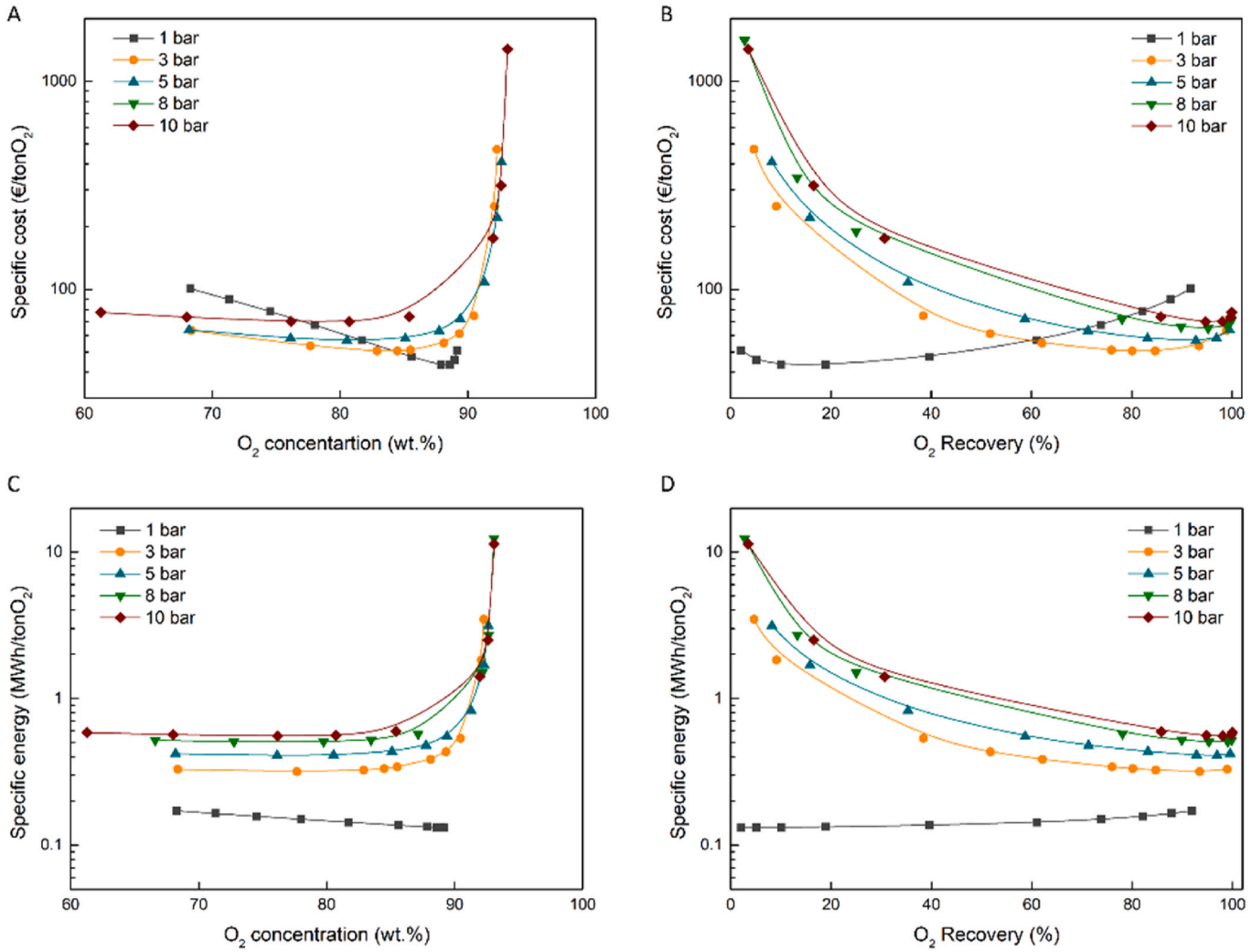


**Fig. 6.** Specific cost of oxygen-enriched air for 5 different feed pressures, for 0.1 bar of permeate pressure, and for an air feed flow rate of 250 tons per day, as a function of the oxygen concentration (A), and as a function of the oxygen recovery (B); energy consumption per mass of produced oxygen as a function of the oxygen concentration C) and as a function of the oxygen recovery (D). The lines were added to guide the eyes.

minimum specific cost of the oxygen-enriched air corresponds to a feed pressure of 3 bar and an oxygen concentration of 88 %, *ca.* 81 €·ton$O_2^{-1}$, *cf.* Fig. 6A. However, when atmospheric feed pressure is considered, it is possible to produce oxygen with a somewhat higher concentration (*ca.* 88 %) at the same specific cost. But in this case, the oxygen recovery is much lower, about 20 %, while for feed pressure of 3 bar the recovery is *ca.* 80 %. It should be emphasized that for low-stage cuts and for a given feed-to-permeate pressure ratio, compressing the feed corresponds to transferring a large amount of energy that will be wasted as compressed retentate. In these cases, it is far more attractive to transfer pressure energy (vacuum in this case) just to the permeated flowrate, since all the applied energy will be used for the permeation.

From the previous optimization, 3 bar of feed pressure guarantees the best relationship between oxygen recovery and concentration, with minimal specific separation cost. The relationship of capital and operating costs (and specific cost) as a function of the oxygen concentration and recovery are shown in Fig. 7A and Fig. 7B, respectively.

As can be seen from Fig. 7A, operational expenses (OPEX) and annual capital costs decrease with increasing oxygen concentration. This behavior is related to two factors: (1) oxygen recovery is lower for high oxygen concentrations, so less permeate flowrate is pumped by the vacuum pump, decreasing its power demand and capital and operational costs; (2) less membrane area is required – Fig. 5. In this process, operating costs are higher than annual capital costs, and the specific oxygen cost is more sensitive to the production flowrate; power demand increases with oxygen recovery. In this case, an optimal specific cost of *ca.* 74.5 €·ton$O_2^{-1}$ is predicted, with a recovery of 80 %, a stage-cut of 0.2, an oxygen concentration of 84.5 %, and a power consumption of 645 kW.

### 5.3. Influence of the produced oxygen concentration on the specific oxygen cost

Two target oxygen concentrations were considered, one typical for combustion enhancement, and the other for medical applications, respectively >70 % and >82 %. Using an oxygen-enhanced air stream increases the $CO_2$ concentration in the flue gas, reducing the eventual capture and purification process costs, and reducing the carbon dioxide emissions making the combustion more efficient [1]. According to the World Health Organization directive, a minimum oxygen concentration of 82 % is required for oxygen therapy or supplemental oxygen [52]. A feed flow rate of 250 ton per day and a permeate pressure of 0.1 bar were assumed in this study.

To determine the minimum specific cost for producing oxygen-enriched air for these two concentrations – 70 % and >82 % – using a single-stage CMSM, it was applied a design of experiments. The pressure ratio and the specific area were varied in the window determined in the previous sections of this work; the pressure ratios were varied between 10 and 100, and the specific area between 40 and 400. The response variables selected are the stage-cut, the oxygen concentration, and the specific cost of producing the oxygen-enrich air stream. A second-order polynomial was used to fit the results from the DoE, and the obtained parameters listed in Table S2 of the supplementary Note 2, along with ANOVA analysis. The empirical polynomial models were considered statistically significant, with *p*-value <0.0001, *p*-value 0.0006, and *p*-value <0.0001, respectively, for the stage-cut, the oxygen concentration, and the specific cost. Model parameters $\beta_4$ and $\beta_5$ displayed for all the dependent variables *p*-values greater than 1 % and were neglected.

Table 2 shows the optimum operating and design conditions for the targeted oxygen concentrations – minimum specific oxygen cost. The results show that the oxygen produced for combustion enrichment applications has a minimum cost of 61 €·ton$O_2^{-1}$ for a stage cut of 0.28 (*i.e.*, 57.2 ton$O_2$·day$^{-1}$) and a pressure ratio of 54; the computed energy consumption is 425 kWh·ton$O_2^{-1}$, the membrane area is 22 425 m$^2$ (90 m$^2$ s·ton$^{-1}$) and the permeated oxygen concentration is 72.8 %.

Regarding oxygen production for medical applications, the optimized has a minimum cost of 45.8 €·ton$O_2^{-1}$ for a stage cut of 0.20 (*i.e.*, 45.6 ton$O_2$·day$^{-1}$) and a pressure ratio of 22; the computed energy consumption is 425 kWh·ton$O_2^{-1}$, the membrane area is 20 700 m$^2$ (83 m$^2$ s·ton$^{-1}$) and the permeated oxygen concentration of 83.5 %. Notably, the cost of producing oxygen at a higher concentration is cheaper. This is because there is an optimum relationship between capital and operating costs and oxygen purity, as observed in other works [53]. Fig. 6 shows that there is a minimum cost for oxygen concentrations between 80 and 90 % (for all the studied pressure ratios).

In section 5.1 of this work, it was concluded that a single CMSM stage it is not enough to produce OEA with a concentration higher than 93.1 %. Oxy-combustion requires, however, an oxygen concentration of ≥95 % [1,13,16,54]. In energy intensive processes such as the production of glass, ceramics, cement or burners, which require very large air feed flowrates (>300 ton$O_2$ per day), cryogenic distillation, with a specific cost of *ca.* 25 €·ton$O_2^{-1}$, is the first choice [18]. However, for processes requiring lower feed flowrates, in the range of 50 ton$O_2$·day$^{-1}$, carbon membranes are expected to be economically feasible. To test this hypothesis, a two-stage carbon membrane process was assumed to reach the required oxygen concentration of >95 %. The operating and design variables of this membrane process were optimized. The lowest specific oxygen cost was obtained for a feed pressure to the first membrane stage of 5 bar (membrane area of 38 225 m$^2$, as concluded in the previous section), and the permeating stream of the first membrane stage needs to

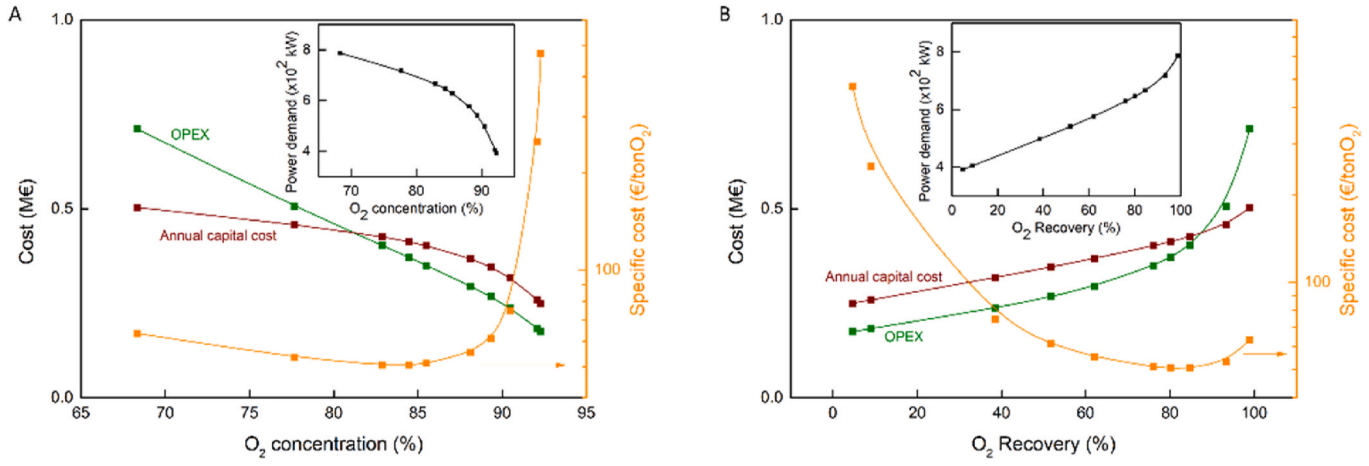


**Fig. 7.** OPEX, annual capital costs, power demand, and oxygen-enriched air-specific production cost as a function of (A) oxygen concentration; and (B) oxygen recovery. The lines were added to guide the eyes.

**Table 2**
Optimal DoE parameters and simulated data.

| | Operating conditions | | Results | | | | |
|---|---|---|---|---|---|---|---|
| | $R$ (−) | Sp. Area ($m^2$·day·$ton^{-1}$) | $\theta$ (−) | $y_{O_2}$ (%) | ACRC (M€) | OPEX (M€) | Sp. Cost (€·$tonO_2^{-1}$) |
| Combustion enhancement | 54 | 90 | 0.28 | 72.8 | 0.52 | 0.65 | 61.0 |
| Medical applications | 22 | 83 | 0.20 | 83.5 | 0.36 | 0.33 | 45.8 |

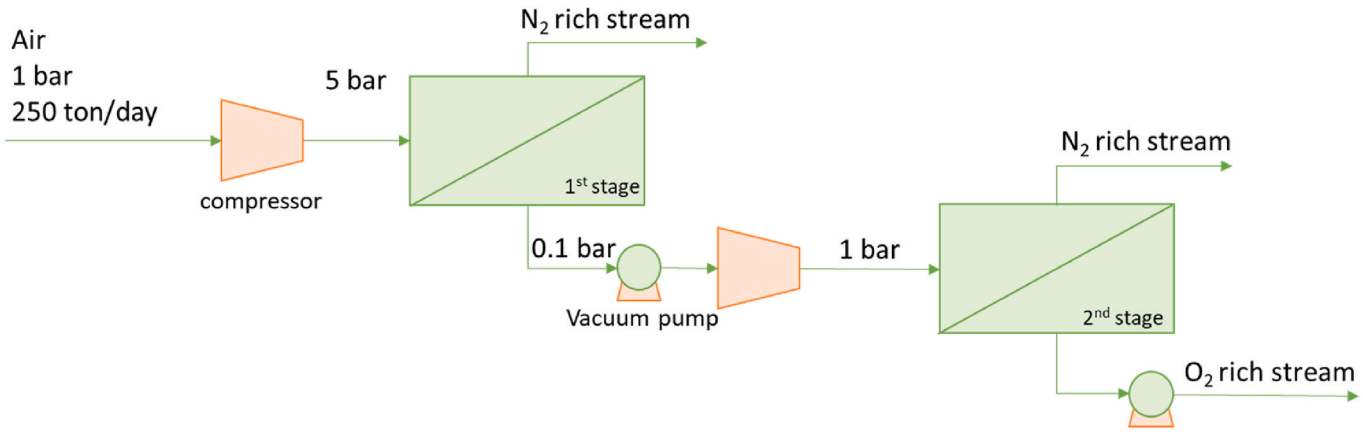


**Fig. 8.** Illustration of the proposed two-stage carbon membrane unit to produce oxygen-enriched air suitable for oxy-combustion (≥95 %).

be compressed at 1 bar to be fed to the second stage (Fig. 8). An oxygen concentration of 95.9 % was obtained at the second CMSM module, with a membrane area of 20 000 $m^2$. The annual capital-related cost (ACRC) of the system was 0.76 M€ and the OPEX was 0.83 M€. The obtained specific oxygen cost was 83.8 €·$tonO_2^{-1}$.

Interestingly, if the system optimized for OEA for medical applications were used as the first CMSM stage, in a two-stage membrane system, it would become possible to produce oxygen with a concentration of 99.3 % in the second stage. The specific cost of producing oxygen at this concentration is 79.1 €·$tonO_2^{-1}$. In this system, the oxygen recovery is 57 %, while for producing the oxygen concentration of 95.9 % is 97 %.

### 5.4. Sensitivity analysis

A sensitive analysis was performed for producing oxygen enriched air with an intermediate concentration (oxygen concentration ≥70 %) suitable for combustion-enhancement and carbon dioxide capture from non-electrified combustion processes (combustion enhancement process) and for oxy-combustion (oxygen concentration ≥95 %).

#### 5.4.1. Membrane thickness

The thickness of the selective layer of the cellulose CMSM was varied from 1 μm to 5 μm for assessing its influence on the specific oxygen cost. As expected, reducing the membrane thickness reduces the specific oxygen cost (Fig. 9A), since the permeance increases and the selectivity stays constant. In this case, the stage cut ($\theta = 0.28$) and pressure ratio ($R = 54$) were kept constant while the required specific area is inversely proportional to the membrane thickness; a specific cost of 53.4 €·$tonO_2^{-1}$ was obtained for a membrane thickness of 1 μm, compared with a specific cost of 61 €·$tonO_2^{-1}$ for a membrane of 3 μm, for producing oxygen-enriched air with 70 %.

#### 5.4.2. Membrane cost

The production cost of the carbon membranes is in the range of 50 €·$m^{-2}$ – 125 €·$m^{-2}$ [31,47,48,53,55]. Cellulose acetate-based carbon membranes were produced semi-industrial by the Norwegian company, MEMFOACT, with a production capacity of 700 $m^2$ $year^{-1}$ [32,56]. This company reported that the production cost of these membranes was 100 €·$m^{-2}$ [32]. This production value can decrease further for higher production rates and with the maturity of the production process. Therefore, an analysis of the production cost of these carbon membranes was performed to determine its influence on the specific oxygen cost. The membrane cost was varied between 25 €·$m^{-2}$ and 125 €·$m^{-2}$; the computed specific oxygen costs are shown in Fig. 9B.

For both oxygen-enriched air separation purities – ≥70 % and ≥95 %, the specific oxygen cost increases with the membrane cost. For example, for a 1 μm thick membrane, when the cost of this membrane decreases from 100 €·$m^{-2}$ to 25 €·$m^{-2}$, the specific oxygen cost for an oxygen concentration of ≥70 %, decreases only 6 %, from 53.4 €·$tonO_2^{-1}$ to 50.4 €·$tonO_2^{-1}$. Regarding the specific cost of the two-stage system for an oxygen concentration >95 %, when the cost of the membrane decreases, there is a reduction in the specific oxygen cost of *ca.* 9 %, from 69.0 to 63.3 €·$tonO_2^{-1}$.

#### 5.4.3. Electricity cost

The cost of electricity directly impacts the specific oxygen cost (Fig. 9C). The cost of electricity in Portugal tends to vary with the price of natural gas (which accounts for *ca.* 40 % of the electricity), even though *ca.* 50 % of the energy produced in Portugal comes from renewable sources [57]. Also, the final electricity price depends on whether the power is produced locally or transmitted using the national high-voltage power grid; if produced locally, its price is substantially lower. When the electricity price changes from 0.15 €·$kWh^{-1}$ to 0.04 €·$kWh^{-1}$, the oxygen production cost drops *ca.* 58 % for a produced oxygen concentration of ≥70 % (80.2 €·$tonO_2^{-1}$ to 33.4 €·$tonO_2^{-1}$), while for an oxygen concentration of ≥95 %, which requires a two-stage membrane system, the production cost drops from 101 €·$tonO_2^{-1}$ to 41 €·$tonO_2^{-1}$, a reduction of *ca.* 59 %.

#### 5.4.4. Project lifetime

The lifetime of the carbon membranes has a significant impact on capital amortization. The CMSMs produced from cellulose using the ionic liquid regenerated approach, post-treated with propylene gas, are very stable for gas separations, as shown in Ref. [58]; CMSMs are far more stable than polymeric membranes, whose average lifetime is just 5 years [5,32,34,47]. Therefore, if 25 years of a lifetime is assumed for the CMSM membranes, instead of 5 years, the annual CAPEX would decrease from 623 k€ to *ca.* 125 k€, for a produced oxygen concentration

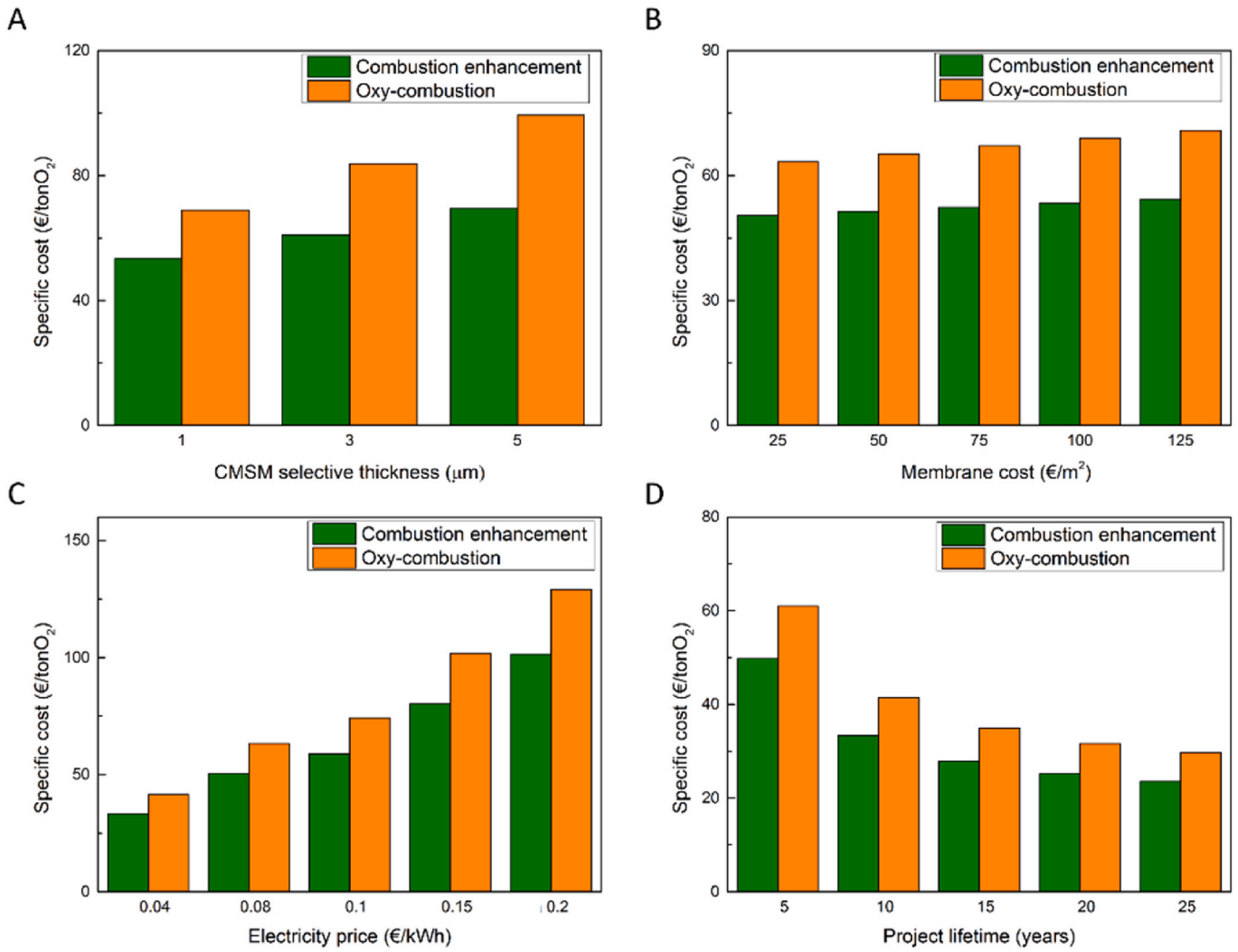


**Fig. 9.** Sensitive analyses of the oxygen-enriched air production cost for two oxygen concentrations: ≥70 % (combustion enhancement) and ≥95 % (oxy-combustion). Sensitivity to: (A) CMSM selective thickness; (B) membrane cost, (C) electricity price, and (D) project lifetime.

of ≥70 %, and the specific oxygen cost would reduce from 49.8 €·tonO$_2^{-1}$ to 23.5 €·tonO$_2^{-1}$. Following, the specific oxygen cost for a produced oxygen concentration of ≥95 % would reduce from 61 €·tonO$_2^{-1}$ to 29.7 €·tonO$_2^{-1}$ – Fig. 9D.

### 5.5. Comparison with other membrane separation processes

Polymeric membranes, particularly those commercialized by Air Products and Chemicals, Inc (Prism®), are used for nitrogen production on an industrial scale [24]. The polymeric membranes from Air Products and from MTR (Polaris™) were used in this work for comparison. The same simulation procedure was used to compute the metrics to produce oxygen for combustion-enhancement (≥70 %) and for oxy-combustion (≥95 %). The polymeric membrane cost was set to 50 €·m$^{-2}$ and the electricity price set to 0.08 €·kWh$^{-1}$, as in the previous studies, and a lifetime of 5 years was assumed. The results of this techno-economic analysis are summarized in Table 3.

The production of oxygen-enhanced air for combustion-enhancement (oxygen concentration ≥70 %) using a single-stage unit is not possible when polymeric membranes are used, due to their low selectivity. Therefore, a unit with two stages of polymeric membranes was considered in this study to compare with the single-stage CMSM unit. The specific cost of producing oxygen at a concentration of >70 % with the Air Products membranes (Prism® membranes) is more than 3 times higher than with the carbon membranes, 61 €·tonO$_2^{-1}$ *vs* 188 €·tonO$_2^{-1}$. Also, the specific required energy for performing the separation increases from 424 kWh·tonO$_2$ to 1189 kWh·tonO$_2^{-1}$. The use of MTR (Polaris™) membranes, which present a higher permeance than

**Table 3**
Comparison of CMSM and commercial polymeric membranes regarding their separation performances and respective costs for producing combustion-enhancement (oxygen concentration ≥70 %) and oxy-combustion (oxygen concentration ≥95 %) grades.

| | Post-combustion (>70 %) | | | Oxy-combustion (>95 %) | | |
|---|---|---|---|---|---|---|
| | CMSM | Prism® | Polaris™ | CMSM | Prism® | Polaris™ |
| **ACRC (k€·year$^{-1}$)** | 517 | 1836 | 2038 | 760 | 3471 | 6247 |
| **OPEX (k€·year$^{-1}$)** | 647 | 1876 | 2285 | 830 | 4363 | 8327 |
| **Cost (€·tonO$_2^{-1}$)** | 61.0 | 188 | 227 | 83.8 | 263 | 353 |
| **Energy (kWh·tonO$_2^{-1}$)** | 425 | 1189 | 1500 | 640 | 1734 | 2446 |

the carbon membranes) but 10 times lower selectivity, was also analyzed. The specific production cost of oxygen-enriched air with MTR membranes is 227 €·ton$O_2^{-1}$ and the specific energy is *ca.* 3 times higher than using carbon membranes.

A three-stage polymer membrane system was considered to produce oxy-combustion grade (oxygen concentration ≥95 %). For the Polaris™ membranes, a maximum oxygen concentration of *ca.* 93 % was obtained, which is below the target. Since for both polymeric membranes, a three-stage membrane process was considered, while the CMSM requires only two stages, the annual capital cost and the energy required are much higher than for the CMSM-based system. The annual capital cost of using Polaris™ membranes is over 6 M€, while using carbon membranes costs *ca.* 517 k€. The OPEX of using Prism® membranes is *ca.* 5 times higher than using carbon membranes; for Polaris membranes, it is *ca.* 9 times higher. With Prism membranes, the specific cost of oxygen is *ca.* 263 €·ton$O_2^{-1}$; and with Polaris membranes, it is *ca.* 4 times higher than for carbon membranes (353 €·ton$O_2^{-1}$). Regarding energy consumption, it is *ca.* 3–4 times higher when the polymeric membranes are used.

For both oxygen-enriched air concentrations, the cellulose-based carbon membranes considered in this work present the lowest capital and operational costs. Assuming a 3 μm membrane thickness, the single-stage CMSM unit presents the lowest separation costs compared with the two commercial polymeric membranes, but also compared with a PSA unit – specific cost of 71 €·ton$O_2^{-1}$ and specific energy of 800 kWh·ton$O_2^{-1}$, for a 300 ton$O_2$·day$^{-1}$ [23]. The CMSM technology is also competitive with the cryogenic distillation – specific cost of 12.4–48 €·ton$O_2^{-1}$ and specific energy of 155–600 kWh·ton$O_2^{-1}$, for a 4000 ton$O_2$·day$^{-1}$ [23], if assumed a membrane thickness of 1 μm, a membrane cost of 25 €·m$^{-2}$, an electricity price of 0.04 €·kWh$^{-1}$ and a capital amortization of ≥10 years. Alternatively, for a CMSM with the same permeance (333 GPU) but with an ideal selectivity of 333, a one-stage membrane unit ($R$ = 10 and $\varphi$ = 240 m$^2$·day·ton$^{-1}$ is sufficient for producing an oxygen current of 95.4 %, displaying a specific cost of just 21.7 €·ton$O_2^{-1}$ and specific energy of 122 kWh·ton$O_2^{-1}$ lower than for the cryogenic distillation. Developing fast and more selective membranes is the continuous objective of this research team, targeting separation costs well below the cryogenic separation.

## 6. Conclusions

This work studies the use of carbon molecular sieve membranes to produce oxygen-enriched air. A phenomenological simulator was developed to solve the mass balance and kinetic equations of a counter-current membrane module based on a simple and intuitive numerical method implemented in Matlab®. It was assumed a CMSM with a permeability to oxygen of 333 barrer, $O_2/N_2$ ideal selectivity of 54, and a membrane thickness of 3 μm.

The relationship between the stage cut, specific membrane area, and oxygen concentration was studied for a constant pressure ratio, assuming a feed pressure of 1 bar. It was concluded that for a given membrane, there is a permeating oxygen concentration that minimizes the specific oxygen cost, which was named nominal oxygen concentration. As expected, the specific oxygen cost decreases as the feed flow rate increases, due to the CAPEX scaling factor. A minimum specific cost for oxygen production of *ca.* 74 €·ton$O_2^{-1}$ was obtained for an air stream of 623 ton·day$^{-1}$ to 87 % oxygen concentration. The impact of the feed-to-permeate pressure ratio was also assessed. For low stage-cuts, it is always better to have just a vacuum pump, which pumps only the permeate stream, than a compressor that has to compress a higher feed flowrate.

The production of oxygen-enriched air for combustion-enhancement, medical applications, and oxy-combustion requires different concentrations, namely 70 %, 82 %, and 95 %. A design of experiments was performed to obtain the operating variables that minimize the specific oxygen cost. The obtained minimum specific oxygen costs for the three oxygen concentrations are 61 €·ton$O_2^{-1}$ for combustion enhancement (≥70 %), 45.8 €·ton$O_2^{-1}$ for medical applications (≥82 %), and 83.8 €·ton$O_2^{-1}$ oxy-combustion (≥95 %). To reach an oxygen concentration of ≥95 %, required for oxy-combustion uses, it was considered a two-stage CMSM process. A sensitivity analysis was performed to assess the contribution to the specific oxygen cost of the membrane thickness, CMSMs production cost and lifetime, and electricity price. It was concluded that the membrane thickness and cost have the lowest impact on the specific oxygen cost. A minimum specific oxygen cost of 29.7 €·ton$O_2^{-1}$ was obtained for an oxygen concentration of 73 % and a membrane thickness of 1 μm; this is an extremely competitive cost. The performed techno-economic analysis is rather simple and aimed to highlight the great potential of the lately developed CMSM for oxygen enrichment.

## CRediT authorship contribution statement

**Tiago Araújo:** Conceptualization, Data curation, Investigation, Methodology, Writing – original draft. **Telmo da Silva Lopes:** Data curation, Investigation, Writing – original draft. **Gabriel Bernardo:** Writing – review & editing, Supervision. **Adélio Mendes:** Conceptualization, Funding acquisition, Project administration, Resources, Supervision, Writing – review & editing.

## Declaration of competing interest

The authors declare that they have no known competing financial interests or personal relationships that could have appeared to influence the work reported in this paper.

## Data availability

Data will be made available on request.

## Acknowledgments

T. Araújo and T. Lopes are grateful to the Portuguese Foundation for Science and Technology (FCT) for the doctoral grants (ref. SFRH/BD/143598/2019 and SFRH/BD/147426/2019) supported by POPH/FSE. G. Bernardo thanks to FCT for the financial support of his work contract through the Scientific Employment Stimulus Individual Call – (CEECIND/02039/2018). This work was financially supported by LA/P/0045/2020 (ALiCE), UIDB/00511/2020 and UIDP/00511/2020 (LEPABE), funded by national funds through FCT/MCTES (PIDDAC).

## Appendix A. Supplementary data

Supplementary data to this article can be found online at https://doi.org/10.1016/j.memsci.2024.122430.

## Nomenclature

*Greek Symbol Definition Unit*

$\beta$ Empiric model equation parameter

| | |
|---|---|
| $\theta$ | Stage cut ($\theta = Q_{permeate}/Q_{feed}$) |
| $\varphi$ | Specific area ($\varphi = A/Q$) $m^2$·day·$ton^{-1}$ |
| $\eta_C$ | Compressor efficiency % |

*Variable, Definition, Unit*

| | |
|---|---|
| $A$ | Membrane area, $m^2$ |
| $C_{ACRC}$ | Annual capital related cost, € |
| $C_{CAPEX}$ | Capital expenditure, € |
| $C_c$ | Compressor cost, € |
| $C_{CEPCI}$ | Chemical engineering plant cost index |
| $c_i$ | Concentration, mol·$m^{-3}$ |
| $C_{vp}$ | Vacuum pump cost, € |
| $D_i$ | Diffusivity coefficient, $m^2$·$s^{-1}$ |
| $F$ | Indirect cost factor, % |
| $F_F$ | Feed molar flow, mol·$s^{-1}$ |
| $F_P$ | Permeate molar flow, mol·$s^{-1}$ |
| $F_R$ | Retentate molar flow, mol·$s^{-1}$ |
| $i$ | Component $i$ |
| $I$ | Inflation adjustment factor |
| $j$ | Component $j$ |
| $k$ | Specific heat ratio |
| $l$ | Membrane thickness, nm |
| $L_i$ | Permeance ($P_i/l$) (1 GPU = $3.35 \times 10^{-10}$ mol $m^{-2}$ $s^{-1}$•$Pa^{-1}$), GPU |
| $OPEX$ | Operational-related expenditure cost, € |
| $P_C$ | Compressor power, kW |
| $P_{discharge}$ | Compressor discharge pressure, Pa |
| $P_i$ | Permeability (1 barrer = $3.39 \times 10^{-16}$ mol m $m^{-2}$·$s^{-1}$ $Pa^{-1}$), barrer |
| $p_i$ | Pressure, Pa |
| $P_p$ | Permeate pressure, Pa |
| $P_R$ | Retentate pressure, Pa |
| $P_{suction}$ | Compressor suction pressure, Pa |
| $P_{vp}$ | Vacuum pump power, kW |
| $Q$ | Volumetric flow rate, mol·$s^{-1}$ |
| $R$ | Pressure ratio ($R = P_{feed}/P_{permeate}$), - |
| $S_i$ | Sorption coefficient, mol·$m^{-3}$·$Pa^{-1}$ |
| $x$ | Feed molar fraction, % |
| $y$ | Permeate molar fraction, % |
| $z$ | Special coordinate |
| $+1$ | Upper level of the DoE factor |
| $-1$ | Lower level of the DoE factor |

## References


[1] M. Micari, K.V. Agrawal, Oxygen enrichment of air: performance guidelines for membranes based on techno-economic assessment, J. Membr. Sci. 641 (2022) 119883.

[2] P. Higginbotham, V. White, K. Fogash, G. Guvelioglu, Oxygen supply for oxyfuel CO2 capture, Int. J. Greenh. Gas Control 5 (2011) S194–S203.

[3] D.J. Dillon, V. White, R.J. Allam, R.A. Wall, J. Gibbins, IEA Greenhouse Gas R&D Programme: Oxy Combustion Processes for CO2 Capture from Power Plant, 2005.

[4] F. Galli, D. Previtali, G. Bozzano, C.L. Bianchi, F. Manenti, C. Pirola, Production and application of O2 enriched air produced by fresh and salt water desorption in chemical plants, J. Environ. Manag. 217 (2018) 621–628.

[5] B. Adhikari, C.J. Orme, J.R. Klaehn, F.F. Stewart, Technoeconomic analysis of oxygen-nitrogen separation for oxygen enrichment using membranes, Separ. Purif. Technol. 268 (2021) 118703.

[6] Elisabeth D. Hasler, S. Saxer, Simon R. Schneider, M. Furian, M. Lichtblau, Esther I. Schwarz, Konrad E. Bloch, S. Ulrich, Effect of breathing oxygen-enriched air on exercise performance in patients with chronic obstructive pulmonary disease: randomized, placebo-controlled, cross-over trial, Respiration 99 (2020) 213–224.

[7] M.W. Ackley, Medical oxygen concentrators: a review of progress in air separation technology, Adsorption 25 (2019) 1437–1474.

[8] Y. Alqaheem, A. AlomaİR, Enriched oxygen for crude oil preheating in petroleum refining, Int. J. Therm. 24 (2021) 128–132.

[9] S. Chin, J. Jurng, J.-H. Lee, J.-H. Hur, Oxygen-enriched air for co-incineration of organic sludges with municipal solid waste: a pilot plant experiment, Waste Manag. 28 (2008) 2684–2689.

[10] T. Miller, J. Jimenez, A. Sharan, D. Goldstein, Oxygen steelmaking processes, the Making, Shaping and Treating of Steel-Steelmaking and Refining ume (1998) 475–524.

[11] V.S. Malik, K. Ravindra, M. Singh, COVID-19 and increasing demand for medical oxygen: can impurity be a problem? Environ. Sci. Pollut. Control Ser. 28 (2021) 66519–66521.

[12] R. Madeline, K.W. Sarah, Oxygen inequity in the COVID-19 pandemic and beyond, Glob. Health Sci. Pract. 11 (2023) e2200360.

[13] H. Lin, M. Zhou, J. Ly, J. Vu, J.G. Wijmans, T.C. Merkel, J. Jin, A. Haldeman, E. H. Wagener, D. Rue, Membrane-based oxygen-enriched combustion, Ind. Eng. Chem. Res. 52 (2013) 10820–10834.

[14] Y. Khalid, M. Wu, A. Silaen, F. Martinez, T. Okosun, B. Worl, J. Low, C. Zhou, K. Johnson, D. White, Oxygen enrichment combustion to reduce fossil energy consumption and emissions in hot rolling steel production, J. Clean. Prod. 320 (2021) 128714.

[15] E. Koohestanian, F. Shahraki, Review on principles, recent progress, and future challenges for oxy-fuel combustion CO2 capture using compression and purification unit, J. Environ. Chem. Eng. 9 (2021) 105777.

[16] T. Burdyny, H. Struchtrup, Hybrid membrane/cryogenic separation of oxygen from air for use in the oxy-fuel process, Energy 35 (2010) 1884–1897.

[17] D.M. Ruthven, S. Farooq, Air separation by pressure swing adsorption, Gas Separ. Purif. 4 (1990) 141–148.

[18] B. Belaissaoui, Y. Le Moullec, H. Hagi, E. Favre, Energy efficiency of oxygen enriched air production technologies: cryogeny vs membranes, Separ. Purif. Technol. 125 (2014) 142–150.

[19] S.F. Douglas, M. Ruthven, Kent S. Knaebel, Pressure Swing Adsorption, Wiley, 1996.

[20] N.O. Lemcoff, Nitrogen separation from air by pressure swing adsorption, in: A. Dąbrowski (Ed.), Studies in Surface Science and Catalysis, Elsevier, 1999, pp. 347–370.

[21] A. Moran, O. Talu, Limitations of portable pressure swing adsorption processes for air separation, Ind. Eng. Chem. Res. 57 (2018) 11981–11987.

[22] S.L. Matson, W.J. Ward, S.G. Kimura, W.R. Browall, Membrane oxygen enrichment: II. Economic assessment, J. Membr. Sci. 29 (1986) 79–96.
[23] S. García-Luna, C. Ortiz, A. Carro, R. Chacartegui, L.A. Pérez-Maqueda, Oxygen production routes assessment for oxy-fuel combustion, Energy 254 (2022) 124303.
[24] R.W. Baker, Membrane Technology and Applications, second ed., ohn Wiley & Sons, Ltd, 2004.
[25] M. Bozorg, B. Addis, V. Piccialli, Á.A. Ramírez-Santos, C. Castel, I. Pinnau, E. Favre, Polymeric membrane materials for nitrogen production from air: a process synthesis study, Chem. Eng. Sci. 207 (2019) 1196–1213.
[26] Y.H. Chu, A. Lindbrathen, L.F. Lei, X.Z. He, M. Hillestad, Mathematical modeling and process parametric study of CO2 removal from natural gas by hollow fiber membranes, Chem. Eng. Res. Des. 148 (2019) 45–55.
[27] I.W. Backhouse, Novel applications for gas separation membranes, in: M.K. Turner (Ed.), Effective Industrial Membrane Processes: Benefits and Opportunities, Springer Netherlands, Dordrecht, 1991, pp. 383–389.
[28] R. Jain, Method for economic evaluation of membrane-based air separation, Gas Separ. Purif. 3 (1989) 123–127.
[29] L.M. Robeson, The upper bound revisited, J. Membr. Sci. 320 (2008) 390–400.
[30] M. Atkinson, J. Barry, M. Ciampini, J. Greene, A. Marker, U.S. Department of Energy, Improving Process Heating System Performance, A Sourcebook for Industry, 2004.
[31] L. Lei, L. Bai, A. Lindbråthen, F. Pan, X. Zhang, X. He, Carbon membranes for CO2 removal: status and perspectives from materials to processes, Chem. Eng. J. 401 (2020) 126084.
[32] S. Haider, A. Lindbråthen, J.A. Lie, M.-B. Hägg, Carbon membranes for oxygen enriched air – Part II: techno-economic analysis, Separ. Purif. Technol. 205 (2018) 251–262.
[33] T. Araújo, A.J. Parnell, G. Bernardo, A. Mendes, Cellulose-based carbon membranes for gas separations - unraveling structural parameters and surface chemistry for superior separation performance, Carbon 204 (2023) 398–410.
[34] X. He, D. Chen, Z. Liang, F. Yang, Insight and comparison of energy-efficient membrane processes for CO2 capture from flue gases in power plant and energy-intensive industry, Carbon Capture Science & Technology 2 (2022) 100020.
[35] D. Grainger, M.B. Hagg, The recovery by carbon molecular sieve membranes of hydrogen transmitted in natural gas networks, Int. J. Hydrogen Energy 33 (2008) 2379–2388.
[36] P. Cruz, J.C. Santos, F.D. Magalhães, A. Mendes, Simulation of separation processes using finite volume method, Comput. Chem. Eng. 30 (2005) 83–98.
[37] D.T. Coker, B.D. Freeman, G.K. Fleming, Modeling multicomponent gas separation using hollow-fiber membrane contactors, AIChE J. 44 (1998) 1289–1302.
[38] D. Grainger, Development of Carbon Membranes for Hydrogen Recovery in, Department of Chemical Engineering, Norwegian University of Science and Technology, Trondheim, 2007, p. 246.
[39] L.F. Shampine, M.W. Reichelt, J. Lkierzenka, Solving Boundary Value Problems for Ordinary Differential Equations in MATLAB with Bvp4c - MATLAB File Exchange, 2004.
[40] Z. Liang, F. Yang, Y. Li, J. Tang, D.R. Dekel, X. He, Designing the feasible membrane systems for CO2 removal from Air-fed Anion-Exchange membrane fuel cells, Separ. Purif. Technol. 289 (2022) 120713.
[41] A. Janusz-Cygan, J. Jaschik, A. Wojdyła, M. Tańczyk, The separative performance of modules with polymeric membranes for a hybrid adsorptive/membrane process of CO2 capture from flue gas, Membranes 10 (11) (2020) 309.
[42] S.C. Rodrigues, M. Andrade, J. Moffat, F.D. Magalhães, A. Mendes, Carbon membranes with extremely high separation factors and stability, Energy Technol. 7 (2019) 1801089.
[43] J. Chen, L.S. Loo, K. Wang, D.D. Do, The structural characterization of a CMS membrane using Ar sorption and permeation, J. Membr. Sci. 335 (2009) 1–4.
[44] M. Campo, F. Magalhães, A. Mendes, Carbon molecular sieve membranes from cellophane paper, J. Membr. Sci. 350 (2010) 180–188.
[45] M. Andrade, S.C. Rodrigues, A. Mendes, High performing CMS adsorbent for O2/N2 separation, Microporous Mesoporous Mater. 296 (2020) 109989.
[46] F. Relvas, R.D. Whitley, C. Silva, A. Mendes, Single-stage pressure swing adsorption for producing fuel cell grade hydrogen, Ind. Eng. Chem. Res. 57 (2018) 5106–5118.
[47] X. He, L. Lei, Z. Dai, Green hydrogen enrichment with carbon membrane processes: techno-economic feasibility and sensitivity analysis, Separ. Purif. Technol. 276 (2021) 119346.
[48] X. He, Y. Chu, A. Lindbråthen, M. Hillestad, M.-B. Hägg, Carbon molecular sieve membranes for biogas upgrading: techno-economic feasibility analysis, J. Clean. Prod. 194 (2018) 584–593.
[49] W.L. Luyben, Capital cost of compressors for conceptual design, Chemical Engineering and Processing - Process Intensification 126 (2018) 206–209.
[50] B.D. Bhide, S.A. Stern, A new evaluation of membrane processes for the oxygen-enrichment of air. I. Identification of optimum operating conditions and process configuration, J. Membr. Sci. 62 (1991) 13–35.
[51] M. Mulder, Membrane processes, in: M. Mulder (Ed.), Basic Principles of Membrane Technology, Springer Netherlands, Dordrecht, 1996, pp. 280–415.
[52] World Health Organization, WHO-UNICEF Technical Specifications and Guidance for Oxygen Therapy Devices, 2019.
[53] S. Haider, A. Lindbrathen, J.A. Lie, M.B. Hagg, Carbon membranes for oxygen enriched air - Part II: techno-economic analysis, Separ. Purif. Technol. 205 (2018) 251–262.
[54] D. Ariono, A.K. Wardani, Review of membrane oxygen enrichment for efficient combustion, J. Phys. Conf. 877 (2017) 012050.
[55] X. He, M.-B. Hägg, Hollow fiber carbon membranes: from material to application, Chem. Eng. J. 215–216 (2013) 440–448.
[56] S. Haider, A. Lindbråthen, J.A. Lie, P.V. Carstensen, T. Johannessen, M.-B. Hägg, Vehicle fuel from biogas with carbon membranes; a comparison between simulation predictions and actual field demonstration, Green Energy Environ. 3 (2018) 266–276.
[57] DGEG/MAAC, PORDATA, Produção bruta de energia elétrica: total e por tipo de produção de energia elétrica, 2023.
[58] T. Araújo, M. Andrade, G. Bernardo, A. Mendes, Stable cellulose-based carbon molecular sieve membranes with very high selectivities, J. Membr. Sci. 641 (2022) 119852.